

# Optical conductivity near finite-wavelength quantum instabilities

S. Caprara, M. Grilli, C. Di Castro, and T. Enss

*SMC-INFM-CNR Rome and Dipartimento di Fisica*

*Università di Roma “La Sapienza”, Piazzale Aldo Moro 5, I-00185 Roma, Italy*

(Dated: February 8, 2020)

We calculate the optical conductivity for a system of quasiparticles coupled to collective modes, which are (nearly) critical at a finite wavevector in the proximity of a quantum critical point. We show that a conserving approximation scheme is crucial to obtain correct results, because the contributions arising from the exchange of critical collective modes are all of the same order. We also show that a non-universal energy scale associated to non-electronic degrees of freedom, responsible for electron momentum dissipation, rules the low-energy response and may mask the effects of the collective modes even when these become fully critical.

PACS numbers: 73.43.Nq, 78.20.-e, 73.20.Mf, 71.45.Lr

Quantum criticality has become a central issue in solid-state physics and might be the crucial ingredient to account for non-Fermi-liquid properties of cuprates [1, 2, 3, 4], heavy fermions [5] and other strongly correlated electron systems. A relevant goal is to determine the role of critical fluctuations in various anomalous properties. In this letter we analyze the optical conductivity *within a fully conserving approach* for the general case of a system near a quantum critical point (QCP) with finite-wavelength order. This general analysis is not only pertinent to the cuprates, where a relevant role of spin- [1] or charge-ordering [2] fluctuations has been proposed, but may apply to all cases (heavy fermions, dichalcogenides, and so on), where quasiparticles (QP’s) are coupled to collective modes (CM’s) becoming critical at a finite wavevector  $\mathbf{q}_c$ . In this case, the Fermi surface is divided into “hot” regions [hot spots (HS’s)] connected by  $\mathbf{q}_c$  and “cold” regions, where energy and momentum conservation do not allow QP’s to exchange low-energy critical fluctuations at  $\mathbf{q} \approx \mathbf{q}_c$ . Contrary to other analyses based on field-theoretical bosonic effective models [6], we start from a microscopic electronic model and focus on *neutral* order parameter fluctuations. In this case, the coupling between the external photon field and the CM’s is non-trivial. Then the optical response function is not directly related to fluctuations of the order parameter and simple scaling properties might be masked by non-universal effects. The issues we address are two: i) to what extent critical excitations, usually characterized by a strong dependence on temperature and other control parameters (like pressure or chemical doping), are visible and produce specific signatures in optical conductivity; ii) how relevant and important it is to adopt a conserving scheme to calculate the effects of point i).

We anticipate here that i) (critical) CM’s may indeed give rise to specific features in optical spectra, but ii) our conserving approach clearly demonstrates that the strong dependencies of the CM’s may be weakened by momentum conservation. Depending on non-universal parameters, the CM peaks may become weakly dispersive, or

disappear at all.

— *The model* — We start from a model effective action at a temperature  $T$

$$\begin{aligned} \mathcal{S} = & T \sum_{\substack{|\mathbf{k}| < \Lambda_f \\ \epsilon_\ell, \sigma}} G_0^{-1}(k) c_{k,\sigma}^\dagger c_{k,\sigma} + T \sum_{\substack{|\mathbf{q}| < \Lambda_b \\ \omega_n}} \chi_0^{-1}(q) \phi_q \phi_{-q} \\ & + T^2 \sum_{\substack{|\mathbf{q}| < \Lambda_b \\ \omega_n}} \sum_{\substack{|\mathbf{k}| < \Lambda_f \\ \epsilon_\ell, \sigma, \sigma'}} \gamma_{\sigma\sigma'}^{s,c} c_{k+q,\sigma}^\dagger c_{k,\sigma'} \phi_{-q} \end{aligned} \quad (1)$$

where  $k \equiv (\mathbf{k}, \epsilon_\ell)$ ,  $q \equiv (\mathbf{q}, \omega_n)$ ,  $\epsilon_\ell$  ( $\omega_n$ ) are fermionic (bosonic) Matsubara frequencies,  $G_0 = (i\epsilon_\ell - \xi_{\mathbf{k}})^{-1}$  is the bare QP propagator,  $\xi_{\mathbf{k}}$  is the band of the QP’s created by the  $c$  fields, and  $\gamma^{s,c}$  is the (theory-dependent) vertex coupling the QP’s to collective charge ( $c$ ) or spin ( $s$ ) excitations, represented by the bosonic fields  $\phi$ .  $\chi_0^{-1}$  is the bare charge or spin susceptibility. At the bare level the  $\phi$  fields mediate an effective electron-electron interaction  $V(q) = \gamma^2 \chi_0(q)$ , which has its own dynamics arising, e.g., from higher-energy (non-critical) spin fluctuations [1], or phonons [2, 7].  $\Lambda_{f,b}$  are ultraviolet cutoffs for fermions and bosons, separating the low-energy QP and critical CM physics from the high-energy physics, where QP band curvature, non-critical behavior of the CM’s, and so on, start to play a non-negligible role. For the sake of concreteness we consider the charge case, where the  $\phi$  fields and the  $\gamma^c$  vertex are scalar, the extension to spin fluctuation being straightforward. To make contact with the case of cuprates and dichalcogenides, we consider the model in two dimensions. The physical in-plane conductivity is then obtained assembling the planes spaced by a distance  $d$ .

To perform a fully conserving calculation we start from a bubble-type Baym-Kadanoff (B-K) functional, whose generic term is exemplified in Fig. 1(a). Once current vertices are inserted, to calculate the conductivity by means of the Kubo formula, the bubble diagrams can be resummed by introducing a RPA-resummed Bose propagator [see Fig. 1(b)]. Then, the full set of conserving diagrams reported in Fig. 1(c) is obtained. These diagrams

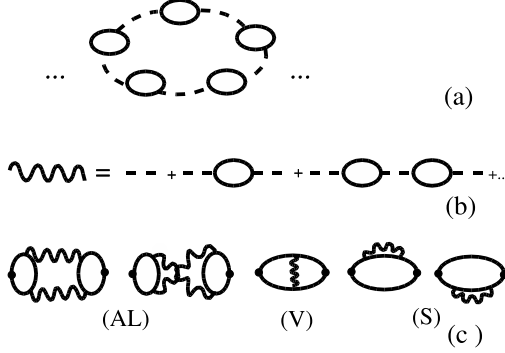


FIG. 1: (a) Typical diagram of the B-K generating functional adopted hereby. The solid and dashed lines represent the QP propagator and the bare interaction  $V(q)$ , respectively. (b) Bubble resummation to obtain the RPA-dressed CM propagator (wavy line). (c) Diagrams for the current-current response, obtained from current-vertex insertions in the diagrams of the B-K functional. The full dots represent the current vertices. AL, V, and S stand for Aslamazov-Larkin-like, vertex and self-energy diagrams, respectively.

give the CM corrections to the bare current-current response. To focus on the effects of critical fluctuations, we neglect disorder. As a consequence, the conductivity still maintains an infinitely narrow  $\delta$ -like Drude term. The critical CM's will produce absorption at finite frequencies.

The RPA-dressed boson-mediated effective interaction arising from the resummation of Fig. 1(b),  $\Gamma = (V^{-1} - \Pi)^{-1}$  [here  $\Pi(q) \equiv -T \sum_k G_0(k+q)G_0(k)$ ], has the generic form

$$\Gamma(q) = -\Gamma_0 \left( m + \nu |\mathbf{q} - \mathbf{q}_c|^2 + |\omega_n| + \omega_n^2 / \bar{\Omega} \right)^{-1}, \quad (2)$$

for  $\mathbf{q} \approx \mathbf{q}_c$  and small frequencies. Except for the  $\omega_n^2$  term, which is crucial in our forthcoming analysis,  $\Gamma(q)$  has the typical form of a propagator for diffusive CM's (damped by QP's) near a Gaussian QCP with dynamical critical index  $z = 2$  [8]. Here  $m$ , proportional to the square of the inverse correlation length, is the CM mass measuring the distance from criticality [9].

The specific form of the coefficients in Eq. (2), which result from the second-order expansion of  $V^{-1} - \Pi$  around  $\mathbf{q}_c$  and  $\omega_n = 0$  is model dependent. In the following we refer to the model developed in Ref. 7, where a bare interaction  $V(q) = V_0(\mathbf{q}) - \lambda \bar{\omega}^2 (\bar{\omega}^2 + \omega_n^2)^{-1}$  was considered, arising from both short- and long-range Coulomb repulsion,  $V_0$ , and from the coupling to a dispersionless phonon of frequency  $\bar{\omega}$ . Here,  $\lambda$  is the electron-phonon coupling. For moderate  $\lambda \lesssim t$ , where  $t$  is the typical electron band energy scale (in cuprates, e.g.,  $t \approx 0.2 - 0.3$  eV), this interaction can lead to a charge-ordering instability, at a wavevector  $\mathbf{q}_c$  [2, 7]. Within this model we find  $\Gamma_0 \equiv \Pi_\omega^{-1}$ ,  $m \equiv \Pi_\omega^{-1} \{ [\lambda - V_0(\mathbf{q}_c)]^{-1} + \Pi_0 \}$ ,  $\bar{\Omega} \equiv \lambda^{-1} \bar{\omega}^2 [\lambda - V_0(\mathbf{q}_c)]^2 \Pi_\omega$ , where  $\Pi_0 \equiv \Pi(\mathbf{q}_c, 0)$ ,  $\Pi_\omega \equiv$

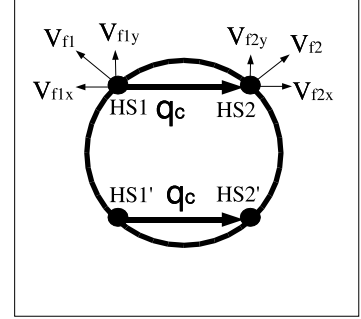


FIG. 2: Sketch of a two-dimensional Fermi surface with four HS's connected by a generic incommensurate critical wavevector  $\mathbf{q}_c = (q_c, 0)$ . Fermi velocities at the HS's and their components are also shown.

$\partial \Pi(\mathbf{q}_c, \omega_n) / \partial \omega_n|_{\omega_n=0}$ . When expanding around  $\mathbf{q}_c$ , an expression like  $\nu_{ij}(\mathbf{q} - \mathbf{q}_c)_i(\mathbf{q} - \mathbf{q}_c)_j$  appears in the expression for  $\Gamma(q)$ . In Eq. (2) we are assuming for simplicity an isotropic form  $\nu_{ij} = \nu \delta_{ij}$ , the generalization being immediate.

In Refs. 2, 7 the instability, signaled by a vanishing mass  $m$ , occurred for values of the parameters such that  $\lambda \sim V_0 \sim |\Pi_0|^{-1} \sim t$ . Then, we estimate  $\nu \sim t$ , and  $\bar{\Omega} \sim \bar{\omega}(\bar{\omega}/t)$ .

— *No momentum dissipation: infinite  $\bar{\Omega}$*  — It is very instructive to consider first the case  $\bar{\Omega} \rightarrow \infty$ , i.e.,  $\bar{\omega} \rightarrow \infty$ . In this case the QP's are only coupled among themselves and with a static phonon field, and the  $\omega_n^2$  term coming from the phonon propagator no longer appears in Eq. (2). As a consequence, the total electron momentum is conserved and the conductivity vanishes for any finite frequency, while only the  $\delta$ -like Drude term remains [11]. To check this important result within an analytic calculation, we adopt the standard procedure of linearizing the QP dispersion around the HS's [1]. In this way, the integrations of the fermionic propagators in the diagrams of Fig. 1(c) can be explicitly carried out. The cancellation results from the relation between  $\Gamma_0 \equiv \Pi_\omega^{-1}$  and the factors arising from the fermionic integrations [12].

It is also interesting to analyze in detail how the different processes related to the diagrams of Fig. 1(c) contribute to the vanishing of the current-current response function,  $\chi_{jj}(\Omega_l) = 0$ . We first consider the response  $\chi_{jj}^{yy}(\Omega_l)$  perpendicular to the critical wavevector (which, as in Fig. 2, we take along the  $x$  direction). In this case, the total AL vertex (with parallel and crossed CM legs, see Fig. 1(c)) entering the AL diagrams vanishes by symmetry, because the arguments  $k_x + q_c$  and  $k_x$  in the  $\mathbf{k}$  integral of the fermionic loop can be interchanged by the change of the variables  $k_x \rightarrow -k_x - q_c$ , without affecting the current vertex  $\propto k_y$ . Then, by changing  $k_y \rightarrow -k_y$ , one obtains exactly the same expression for the vertex, but with an overall minus sign, which proves the vanishing of the vertex. Then, the cancellation of  $\chi_{jj}^{yy}$  oc-

cers between the S and the V diagrams alone. This is reminiscent of the case of a singular forward interaction [13]. Quite different is the case of response parallel to  $\mathbf{q}_c$ ,  $\chi_{jj}^{xx}(\Omega_l)$ . In this case the  $x$  component of the velocities is opposite at HS's connected by  $\mathbf{q}_c$  (see Fig. 2) and the S and V diagrams sum instead of canceling each other. The total cancellation is then recovered by means of the AL diagrams, which now no longer vanish. Indeed, the symmetry arguments used above do not work for the response parallel to  $\mathbf{q}_c$ , because the change of variables also changes the current vertex  $\propto k_x$ , leading to a different expression. The total AL vertex with an incoming photon vertex at zero momentum and frequency  $\Omega_l$  and two outgoing CM legs with momenta and frequencies  $(\mathbf{q}_c, \omega_n + \Omega_l)$  and  $(-\mathbf{q}_c, -\omega_n)$  is (see also Ref. 14)

$$\Gamma_{AL} = 2\pi i J k_{HS,x}^2 \Omega_l^{-1} (|\Omega_l + \omega_n| - |\omega_n|). \quad (3)$$

Here,  $J \sim 1/v_F^2$  is a Jacobian determinant used to change the fermionic momentum integration from the  $k_x, k_y$  variables to the  $\xi_k^1$  and  $\xi_k^2$  fermionic dispersions around HS1 and HS2,  $v_F$  is the Fermi velocity and  $k_{HS,x}$  is the  $x$  component of the Fermi momentum of the HS's [1, 12]. The important lesson to draw from this first analysis is that *the AL contribution is very important and of the same order of the S and V terms*, since it is responsible for the cancellation implementing momentum conservation.

— *Momentum dissipation: finite  $\bar{\Omega}$*  — A response at finite frequency is instead obtained when, e.g., the effect of a dynamical phonon is taken into account [via the  $\omega^2/\bar{\Omega}$  term in Eq. (2)], because in this case there are non-electronic dynamical degrees of freedom, which dissipate the electron momentum.  $\chi_{jj}^{yy}(\Omega_l)$  still vanishes for the symmetry reasons discussed above. However, the response parallel to  $\mathbf{q}_c$ , which in the following we indicate with  $\chi_{jj}$  for brevity, is no longer zero. After analytic continuation of the external Matsubara frequency, we find

$$\begin{aligned} \chi_{jj}(\Omega) &= \frac{A}{(i\Omega - \bar{\Omega})\Omega} P \int_{-\infty}^{+\infty} \frac{dz}{i\pi} \log \left[ \frac{z^2 - \bar{\Omega}(\Lambda_b - iz)}{z^2 - \bar{\Omega}(m - iz)} \right] \\ &\times \left[ \frac{\bar{\Omega}\Omega + i(2z + \Omega)(z - \Omega)}{\bar{\Omega} - i(2z + \Omega)} \coth \left( \frac{z}{2T} \right) \right. \\ &\left. - \frac{i(2z - \Omega)(z - \Omega)}{\bar{\Omega} - i(2z - \Omega)} \coth \left( \frac{z - \Omega}{2T} \right) \right], \end{aligned} \quad (4)$$

where  $A = e^2 v_F^2 / \nu a^2 d$  is the dimensional prefactor. Extracting the conductance quantum  $e^2/\hbar$  and the factor  $1/d$ , which translates the two-dimensional response into the in-plane response of a layered system, we are left with a dimensional factor which we estimate as  $\hbar v_F^2 / \nu a^2 \sim t/\hbar$ .

One can check that  $\text{Im } \chi_{jj}(\Omega)$  linearly vanishes with  $\Omega$ , giving a finite optical conductivity  $\sigma(\Omega) = \text{Im } \chi_{jj}(\Omega)/\Omega$ , for  $\Omega \rightarrow 0$ . However, in our calculation without disorder, a  $\delta$ -like Drude term  $[D_0 - \pi \text{Re } \chi_{jj}(0)]\delta(\Omega)$  is still present, where  $D_0$  is the QP Drude weight

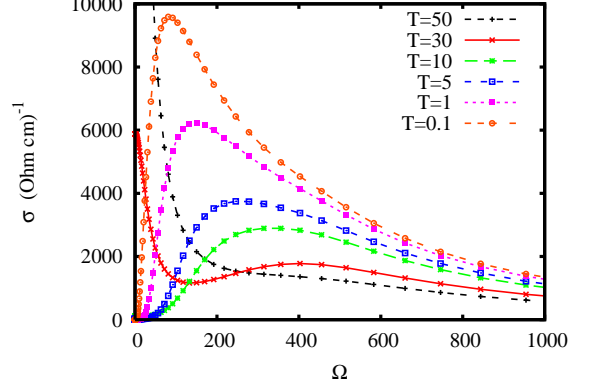


FIG. 3: (Color online) Optical conductivity for a system of QP's coupled to CM's in the quantum-critical regime ( $x = x_{QCP}$ ), with  $m = 30T$  and  $\bar{\Omega} = 30 \text{ cm}^{-1}$ . All frequencies and temperatures are in  $\text{cm}^{-1}$ . The interlayer distance was taken as  $d = 10^{-9} \text{ m}$ .

in the absence of the CM contribution. Kramers-Kronig relations connecting  $\text{Re } \chi_{jj}$  and  $\text{Im } \chi_{jj}$  guarantee spectral weight conservation within our conserving approach: the finite-frequency weight associated with  $\sigma(\Omega)$  is exactly subtracted from  $D_0$  by  $\pi \text{Re } \chi_{jj}(0)$ , i.e.,  $\int d\Omega \{ [D_0 - \pi \text{Re } \chi_{jj}(0)] \delta(\Omega) + \sigma(\Omega) \} = D_0$ .

The  $z$  integration in Eq. (4) is carried out numerically. We find that the  $\bar{\Omega}$  dependence is crucial, not only because  $\chi_{jj}$  vanishes when  $\bar{\Omega} \rightarrow \infty$ , but also because it introduces a natural energy scale in the absorption. This is the main result of this work, because it shows that a non-universal energy scale appears in the optical spectra, which may strongly alter their dependence on the CM mass.  $\bar{\Omega}$  (which we estimated within the model of Refs. [2, 7] as a rather low energy scale  $\sim \bar{\omega}^2/t$ ) determines at low  $T$  the frequency below which momentum conservation leads to a substantial cancellation of absorption. Intuitively, for  $\Omega \ll \bar{\Omega}$ , the response tends to be vanishingly small, as it was for  $\bar{\Omega} = \infty$ . On the other hand, for  $\Omega \gtrsim \bar{\Omega}$  a finite absorption is found even for  $T \rightarrow 0$ . Figs. 3 and 4 report two cases of a system in the quantum critical regime where the mass  $m(x, T) = \alpha T$  can be larger or smaller than  $\bar{\Omega}$ . In the first case (Fig. 3) as long as  $m(T, x) \gtrsim \bar{\Omega}$  the peak position is ruled by  $m$  and the strong  $T$  and  $x$  dependencies of the CM mass are visible as dispersing peaks in the conductivity: the peaks soften and sharpen upon decreasing  $T$ . At finite temperature thermal effects tend to fill the spectra below the peaks and these are clearly visible only if the CM mass, (i.e. the peak frequency), is substantially larger than  $T$ . This is not difficult in the low- $T$  quantum-disordered regime. In the quantum-critical region, where  $m = \alpha T$ , we find instead that absorption peaks become clearly visible at frequencies  $\Omega \sim m(x, T)$  only if the non-universal coefficient  $\alpha \gtrsim 10$ . This condition is satisfied in Fig. 3, where we choose  $m = 30T$ . On the other hand, in Fig. 4 we take  $m(T, x) = 3T \lesssim \bar{\Omega} \approx 330 \text{ cm}^{-1}$  and the peak position is

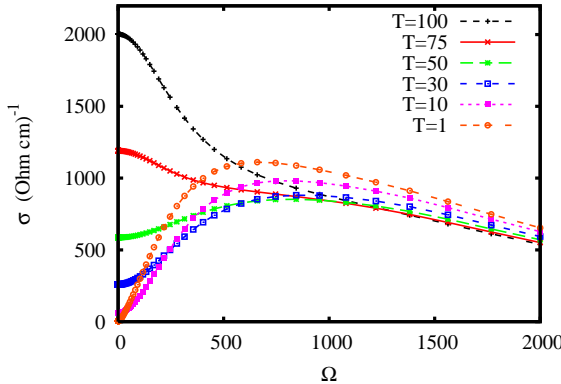


FIG. 4: (Color online) Same as Fig. 3, but with  $m = 3T$  and  $\bar{\Omega} = 330 \text{ cm}^{-1}$ .

ruled by  $\bar{\Omega}$ . In this case, for  $T > 50 \text{ cm}^{-1}$  thermal effects give a CM contribution to the conductivity at low frequency at the expense of the (here unobservable) Drude term. Then the peaks are embedded in this thermally-generated absorption at low frequency and are invisible or, at most, appear as shoulders. Only at  $T \lesssim 0.25\bar{\Omega}$  a peak is visible. This shows that the absence of well-separated absorption peaks in the far infrared optical spectra does not necessarily mean that CM's contributing to the conductivity are absent.

We would like to stress an important point about the position of the peaks: a peak at finite frequency does not necessarily imply a finite CM mass if  $m(T, x) \ll \bar{\Omega}$ . This situation may, e.g., arise at the critical point  $x = x_{QCP}$  where the mass vanishes for  $T \rightarrow 0$  and the regime  $m(T, x) < \bar{\Omega}$  is eventually reached. In this case, as shown in Fig. 4, the peak intensity saturates, and the peak stays pinned at a frequency  $\Omega \sim \bar{\Omega}$  and no longer changes upon further decreasing  $T \propto m$ .[18] This saturation, which occurs even when the CM mass vanishes with  $T$ , is an intrinsic feature of momentum conservation. Therefore, it occurs irrespective of other extrinsic mechanisms (e.g., pinning) which would directly act on the mass  $m$ , keeping it finite. Such extrinsic mechanisms are often present in real systems, but it is crucial to recognize that the saturation of the peak in far infrared spectra may also be an intrinsic phenomenon and cannot be used as evidence against criticality.

— *Discussion* — Our treatment refers to clean systems, but also provides reliable results for dirty systems in the frequency range above the typical impurity scattering rate  $1/\tau$ . In assessing the results discussed above, we strongly relied on a conserving scheme to calculate the optical conductivity. The relevance of vertex corrections was previously proposed [15]. In this letter we provide quantitative evidence that non-conserving approaches may yield qualitatively wrong results. In particular, extensive studies [16] have been carried out considering only S diagrams. It is important to be aware that qualitatively reliable results may only be obtained

for frequencies above  $\bar{\Omega}$ , where the V and AL diagrams do not qualitatively modify the spectra.

Our main result is that optical absorption at finite frequency only appears when electrons are coupled to other dynamical degrees of freedom, allowing for electron momentum dissipation. This introduces a non-universal energy scale  $\bar{\Omega}$ . If  $m > \bar{\Omega}$  the position of the peak due to CM's is ruled by  $m$  and follows the  $x$  and  $T$  dependence of  $m$ . Otherwise, the peak is pinned at a frequency  $\bar{\Omega}$ . Thermal filling effects reduce the visibility of the CM peaks to the regimes where the peak frequency is substantially larger than  $T$ . Whenever the above conditions are not fulfilled, the CM's provide broad absorption or even a peak around zero frequency. In real systems, such absorption would interplay with the Drude peak and could be confused with an additional impurity broadening. Of course, for an explicit quantitative analysis of the optical conductivity at low frequencies, a proper treatment of disorder is needed, which is presently in progress.

In conclusion, in the presence of a QCP (with scaling order-parameter correlations and universality), the conductivity does not need to display a full scaling behavior. Therefore the absence of its scaling behavior cannot be used as evidence against conventional quantum criticality [17].

— *Acknowledgments* — We thank C. Castellani and J. Lorenzana for interesting discussions and acknowledge financial support from the MIUR-PRIN 2005 - prot. 2005022492 and from the Alexander von Humboldt foundation.

---

- [1] A. Abanov *et al.*, *Advances in Physics* **52**, 119 (2003).
- [2] C. Castellani *et al.*, *Phys. Rev. Lett.* **75**, 4650 (1995); *J. of Phys. and Chem. of Sol.* **59**, 1694 (1998).
- [3] C. M. Varma, *Phys. Rev. Lett.* **83**, 3538 (1999).
- [4] C. J. Halboth and W. Metzner, *Phys. Rev. Lett.* **85**, 5162 (2000).
- [5] P. Coleman, *Physica B* **259-261**, 353 (1999).
- [6] See, e.g., K. Damle and S. Sachdev, *Phys. Rev. B* **56**, 8714 (1997), and references therein.
- [7] G. Seibold *et al.*, *Eur. Phys. J. B* **13**, 87 (2000).
- [8] J. A. Hertz, *Phys. Rev. B* **14**, 1165 (1976); A. J. Millis, *Phys. Rev. B* **48**, 7183 (1993).
- [9] Within logarithmic accuracy, in two dimensions in the quantum-critical region  $m \sim T$ , while in the quantum-disordered region  $m \sim (x - x_{QCP})$  (here  $x$  is the control parameter, e.g. doping or pressure, ruling the distance from the QCP). Strictly speaking, corrections beyond RPA must be introduced to produce the correct  $m \sim T$  dependence. However, since the  $T$  dependence of  $m$  is immaterial in the cancellation discussed below, we keep the more physical linear dependence (see, e.g., Ref. 10).
- [10] S. Andergassen *et al.*, *Phys. Rev. Lett.* **87**, 056401 (2001).
- [11] A similar finding within a conserving scheme was discussed for paraconductivity by V. Ambegaokar, in *Superconductivity*, edited by P.R. Wallace (Gordon and

Breach, New York, 1969).

[12] S. Caprara *et al.*, unpublished.

[13] See, e.g., W. Metzner *et al.*, Adv. Phys. **47**, 317 (1998).

[14] B. R. Patton and L. J. Sham, Phys. Rev. Lett. **33**, 638 (1974); E. Sakai and S. Takada, Phys. Rev. B **20**, 2676 (1979).

[15] H. Kontani *et al.*, Phys. Rev. B **59**, 14723 (1999); A. J. Millis and H. D. Drew, Phys. Rev. B **67**, 214517 (2003).

[16] P. Cásek *et al.*, Phys. Rev. B **72**, 134526 (2005); F. Mar-siglio *et al.*, Phys. Lett. A **245**, 172 (1998); S. V. Dordevic *et al.*, Phys. Rev. B **71**, 104529 (2005).

[17] D. van der Marel *et al.*, Nature **425**, 271 (2003); P. Phillips and C. Chamon, Phys. Rev. Lett. **95**, 107002 (2005).

[18] This saturation, of course, also occurs in Fig. 3 where, however, owing to the low value of  $\bar{\Omega}$  the saturation regime is only found at very low temperatures.